

# The Effects of Covalent Ligands on the Oxidative Addition Reaction between Second-Row Transition-Metal Atoms and Methane

Per E. M. Siegbahn,\* Margareta R. A. Blomberg, and Mats Svensson

Contribution from the Department of Physics, University of Stockholm, Box 6730, S-11385 Stockholm, Sweden

Received October 13, 1992

**Abstract:** Calculations including electron correlation of all valence electrons have been performed to study covalent ligand effects in the oxidative addition reaction of methane to second-row transition-metal complexes. Both reaction energies and barrier heights have been determined. As a comparison the reaction energies for the oxidative addition of the hydrogen molecule have also been evaluated. The entire sequence of second-row transition metals from yttrium to palladium has been studied. Hydrogen ligands have been added to systematically saturate all valencies of each metal, which means that results for 23 different reactions each for the oxidative addition of methane and of molecular hydrogen have been obtained. The results are analyzed in terms of promotion energies, loss of exchange energies, and steric and other electronic repulsion effects. The lowest barrier for the methane reaction is found for RuH<sub>2</sub> while the largest exothermicity occurs for ZrH<sub>2</sub>.

## I. Introduction

Because of its fundamental significance and potential technical importance, the C-H activation reaction of alkanes by transition-metal complexes is an important reaction to understand. This reaction was observed for the first time only 10 years ago by Bergman and co-workers<sup>1</sup> for certain iridium complexes. Since then this reaction has been observed to occur also for some other complexes but only for a few different transition metals. These metals are rhodium, iron, osmium, rhenium and iridium.<sup>2-5</sup> It thus appears that very special electronic structure requirements of the metals have to be fulfilled to achieve the C-H activation. There are essentially two different theoretical approaches toward the understanding of this reaction. The first approach, which is the more traditional one, is to make detailed studies of the particular complexes which have been found to be active experimentally.<sup>6-8</sup> The other approach, which has been more recently started, is to build up a systematic, piece by piece understanding of the reaction.<sup>9-11</sup> The first step in this approach is to study the reaction between methane and the naked transition-metal atoms by themselves without ligands. Both theoretically

and experimentally, it has been found that the atomic spectra of the metal atoms play a key role in their reactivity.<sup>9-12</sup> The most systematic way to understand the importance of these electronic structure aspects is to study the reactivity for sequences of transition-metal atoms, each one with its particular electronic spectrum. As a first example of this general strategy, we have recently presented the results for the reaction between the entire second row of the transition-metal atoms and methane.<sup>13</sup> Precursor complexes, transition states, and insertion products of the reaction were studied. In the present paper, which is a natural continuation of the study in ref 13, the effects on the methane reaction from adding covalently bound ligands on the metal are studied. For each metal atom the covalency is systematically saturated. As a parallel, the results for the H<sub>2</sub> addition reaction for the same metal complexes are also presented.

Three main conclusions concerning the electronic structure aspects emerge from the previous theoretical studies of the reaction between the naked transition metal atoms and methane.<sup>9,10,13</sup> First, the main state involved in the binding in the insertion products is the s<sup>1</sup> state (or longer, the d<sup>n+1</sup>s<sup>1</sup> state). For the second-row atoms to the left, there are also important contributions from s<sup>1</sup>p<sup>1</sup> states (or longer, d<sup>n</sup>s<sup>1</sup>p<sup>1</sup> states). The second main conclusion is that at the transition state the s<sup>0</sup> state (or longer, the d<sup>n+2</sup> state) plays a key role. It is the presence of this low-lying state that leads to the lowest barriers for the atoms to the right: ruthenium, rhodium, and palladium. In particular, the lowest barrier of the second-row atoms is found for rhodium since this atom has both low-lying s<sup>0</sup> and s<sup>1</sup> states. It is interesting to note in this context that rhodium complexes are the only second-row complexes which have been found to activate alkanes.<sup>2-5</sup> The third main conclusion concerns the loss of exchange energy<sup>11,13,14</sup> in the reaction. This energy loss is particularly large for the atoms in the middle of the row since there is a large number of

(1) (a) Janowicz, A. H.; Bergman, R. G. *J. Am. Chem. Soc.* **1982**, *104*, 352. (b) Janowicz, A. H.; Bergman, R. G. *J. Am. Chem. Soc.* **1983**, *105*, 3929.

(2) (a) Hoyano, J. K.; Graham, W. A. G. *J. Am. Chem. Soc.* **1982**, *104*, 3723. (b) Hoyano, J. K.; McMaster, A. D.; Graham, W. A. G. *J. Am. Chem. Soc.* **1983**, *105*, 7190.

(3) Jones, W. D.; Feher, F. J. *J. Am. Chem. Soc.* **1982**, *104*, 4240.

(4) Sakakura, T.; Sodeyama, T.; Sasaki, K.; Wada, K.; Tanaka, M. *J. Am. Chem. Soc.* **1990**, *112*, 7221.

(5) *Perspectives in the Selective Activation of C-H and C-C Bonds in Saturated Hydrocarbons*; Meunier, B., Chaudret, B., Eds.; Scientific Affairs Division-NATO: Brussels, 1988.

(6) Koga, N.; Morokuma, K. *J. Phys. Chem.* **1990**, *94*, 5454.

(7) Ziegler, T.; Tschinke, V.; Fan, L.; Becke, A. D. *J. Am. Chem. Soc.* **1989**, *111*, 9177.

(8) Song, J.; Hall, M. B., private communication.

(9) (a) Blomberg, M.; Brandemark, U.; Pettersson, L.; Siegbahn, P. *Int. J. Quantum Chem.* **1983**, *23*, 855. (b) Blomberg, M. R. A.; Brandemark, U.; Siegbahn, P. E. M. *J. Am. Chem. Soc.* **1983**, *105*, 5557. (c) Blomberg, M. R. A.; Schüle, J.; Siegbahn, P. E. M. *J. Am. Chem. Soc.* **1989**, *111*, 6156. (d) Blomberg, M. R. A.; Siegbahn, P. E. M.; Nagashima, U.; Wennerberg, J. *J. Am. Chem. Soc.* **1991**, *113*, 476. (e) Blomberg, M. R. A.; Siegbahn, P. E. M.; Svensson, M. *J. Phys. Chem.* **1991**, *95*, 4313. (f) Blomberg, M. R. A.; Siegbahn, P. E. M.; Svensson, M. *New J. Chem.* **1991**, *15*, 727.

(10) (a) Low, J. J.; Goddard, W. A., III *J. Am. Chem. Soc.* **1984**, *106*, 8321. (b) Low, J. J.; Goddard, W. A., III *Organometallics* **1986**, *5*, 609. (c) Low, J. J.; Goddard, W. A., III *J. Am. Chem. Soc.* **1984**, *106*, 6928. (d) Low, J. J.; Goddard, W. A., III *J. Am. Chem. Soc.* **1986**, *108*, 6115.

(11) (a) Bauschlicher, C. W., Jr.; Langhoff, S. R.; Partridge, H.; Barnes, L. A. *J. Chem. Phys.* **1989**, *91*, 2399. (b) Rosi, M.; Bauschlicher, C. W., Jr.; Langhoff, S. R.; Partridge, H. *J. Phys. Chem.* **1990**, *94*, 8656.

(12) Armentrout, P. B. In *Selective Hydrocarbon Activation: Principles and Progress*; Davies, J. A., Watson, P. L., Greenberg, A., Liebman, J. F., Eds.; VCH Publishers: New York, 1990; pp 467-533.

(13) (a) Svensson, M.; Blomberg, M. R. A.; Siegbahn, P. E. M. *J. Am. Chem. Soc.* **1991**, *113*, 7077. (b) Blomberg, M. R. A.; Siegbahn, P. E. M.; Svensson, M. *J. Am. Chem. Soc.* **1992**, *114*, 6095. (c) Siegbahn, P. E. M.; Blomberg, M. R. A.; Svensson, M. *J. Am. Chem. Soc.* **1993**, *115*, 1952.

(14) Carter, E. A.; Goddard, W. A., III *J. Phys. Chem.* **1988**, *92*, 5679.

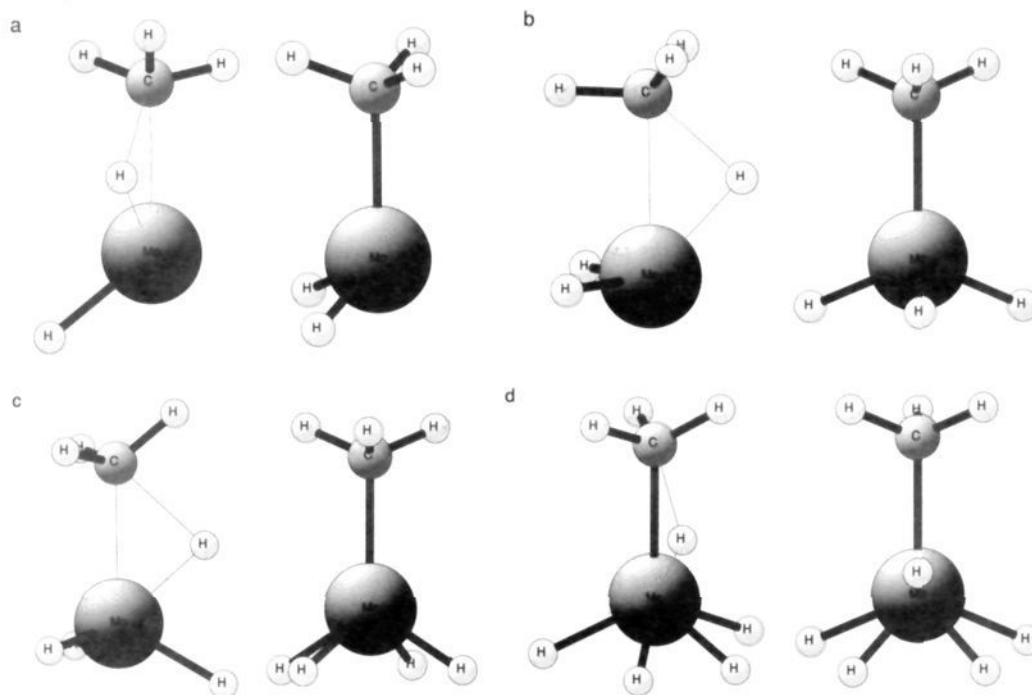


**Figure 1.** Structure of the transition state and the insertion product for the reaction between  $\text{CH}_4$  and (a)  $\text{MoH}$ , (b)  $\text{MoH}_2$ , (c)  $\text{MoH}_3$ , and (d)  $\text{MoH}_4$ .

unpaired 4d electrons for these atoms. Therefore, the binding energies between naked metal atoms and practically any ligand will display a marked minimum in the middle of the row.

The main motivation for choosing covalently bound ligands for the present study is connected to the exchange energy loss mentioned above. For every covalently bound ligand added to the metal, the exchange energy loss in the oxidative addition reaction will decrease. If this was the only effect from adding these ligands, one should expect both lower addition barriers and more strongly bound products as more ligands are added. It is interesting to note that for the rhodium complexes which have been observed to activate alkanes, all valencies have been saturated in line with these arguments. For rhodium complexes this means complexes with valency I, i.e.  $\text{Rh(I)}$  complexes, since two valencies have to be reserved for the alkyl group and the hydrogen atom of the dissociated alkane. It should be added that the important point is that the spin state of the metal is reduced by the addition of ligands, and the simplest way to achieve this is to add covalently bound ligands. The lowering of the spin can also occur when lone pair ligands are added. For example, when  $\text{CO}$  is added to the nickel atom the spin is reduced from triplet to singlet. However, the addition of lone pair ligands will not lead to such a systematic lowering of the spin as when covalent ligands are added.

## II. Results and Discussion

Four different aspects of the present results are discussed below in different subsections. In the first section general aspects are presented such as ground-state electronic states and optimized geometries. In the second section the results for the oxidative addition of  $\text{H}_2$  are presented. Since the barrier heights for this reaction are expected to be either zero or very small, no attempt was made to determine the transition states. In the third subsection, the results for the methane reaction are discussed. In this case geometries and energies for both insertion products and transition states were obtained. Finally, in the fourth subsection, an analysis of all the results is given in terms of exchange effects, steric repulsions, and interactions between nonbonding electrons.

**(a) Geometries and Electronic Ground States.** The geometries of typical methyl hydride complexes, both equilibrium and

**Table I.** Ground-State Spin ( $2S + 1$ ) for the  $\text{MH}_x$  Systems<sup>a</sup>

metal (M)	$x =$						
	0	1	2	3	4	5	6
Y	2(p)	1(p)	2	1			
Zr	3(p)	2(p)	3	2	1		
Nb	6	5	4	3	2	1	
Mo	7	6	5	4	3	2	1
Tc	6	5	6	5	2	1	
Ru	5	4	3	2	1		
Rh	4	3	2	1			
Pd	1(p)	2	1				

<sup>a</sup> The systems which have to be promoted for the reaction between  $\text{MH}_x$  and  $\text{H}_2$  are marked with (p).

transition-state geometries, are given in Figure 1. The corresponding hydride complexes have in most cases the same general structure with the methyl group exchanged with a hydrogen atom, the only exceptions occur for the five-coordinated complexes, as discussed below. The ground-state spins of the hydride complexes (which are the same as for the corresponding methyl hydride complexes) are given in Table I. The geometries given in Figure 1 are the ones that occur for most metals. Cases where other topological structures are found are given in Figure 2 together with some additional structures that are discussed in the text below. The metal complexes for which an electronic promotion to an excited state is needed for the oxidative addition reaction are marked in Table I with the letter p.

In the oxidative addition reaction of  $\text{H}_2$  or  $\text{CH}_4$  two new covalent bonds to the metal are formed. To form these bonds the reactant complex should be in a spin state which is two units higher than the products. If this requirement is not fulfilled the reactant has to be promoted to an excited state. This situation occurs for only a few of the systems studied, the Y, Zr, and Pd atoms and YH and ZrH. It should be added that the technetium complexes represent special examples with a quite irregular variation of ground spin state and these complexes are therefore excluded from most of the present analysis. Apart from these few exceptions, the ground states of the metal complexes behave in a very regular way. For example, for molybdenum the ground-state atom is a septet state and the spin decreases by one unit for every hydrogen atom added until all valencies are saturated for

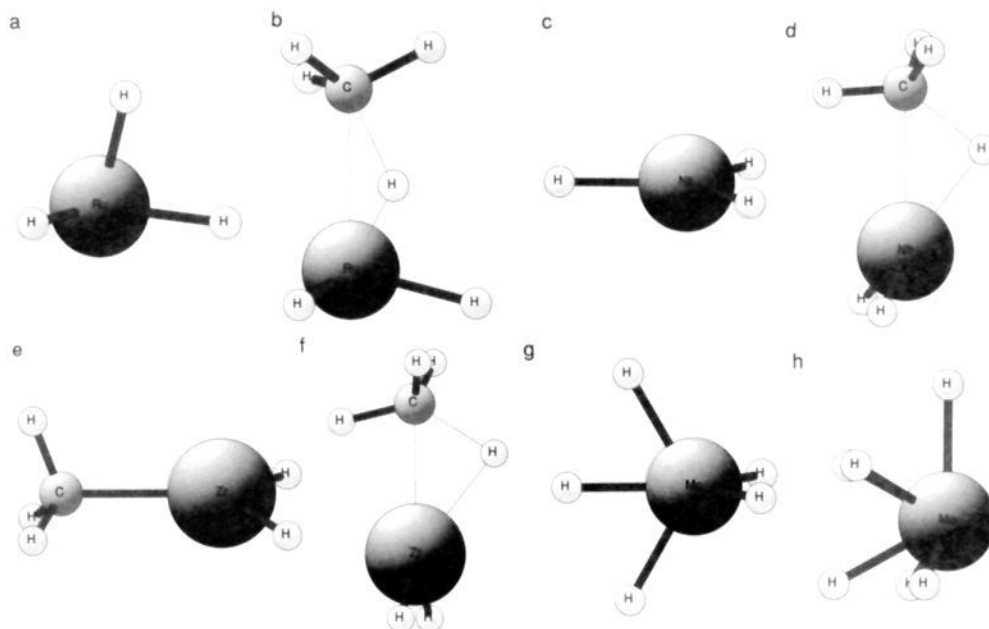


**Figure 2.** (a) Structure of the  $\text{RuH}_3$  complex. (b) Structure of the transition state for the reaction between  $\text{CH}_4$  and  $\text{RuH}_2$ . (c) Structure of the  $\text{NbH}_3$  complex. (d) Structure of the transition state for the reaction between  $\text{CH}_4$  and  $\text{NbH}_2$ . (e) Structure of the  $\text{ZrH}_2\text{CH}_3$  complex. (f) Structure of the transition state for the reaction between  $\text{CH}_4$  and  $\text{ZrH}_2$ . (g) Structure of the  $\text{MoH}_5$  complex. (h) Structure of the  $\text{MoH}_6$  complex.

$\text{MoH}_6$ , which is then a singlet state. The largest promotion energy occurs for the yttrium atom with 34.1 kcal/mol (1.48 eV) from the  $^2\text{D}(d^1s^2)$  state to the  $^4\text{F}(d^2s^1)$  state. For yttrium there is another low-lying  $^4\text{F}$  state, with occupation  $d^1s^1p^1$ , with a calculated excitation energy of 39.7 kcal/mol (1.72 eV). The presence of two close lying promoted states for yttrium has consequences for the analysis below in that the effective promotion energy will appear lower than it actually is. The zirconium atom has a promotion energy of 14.4 kcal/mol (0.62 eV) and the palladium atom one of 20.3 kcal/mol (0.88 eV). The diatomic  $\text{YH}$  is a  $^1\Sigma^+$  state and needs to be promoted to the  $^3\Delta$  state with an excitation energy of 21.6 kcal/mol (0.93 eV), and finally a small promotion energy of 2.4 kcal/mol (0.10 eV) is needed to promote the  $^2\Delta$  state of  $\text{ZrH}$  to the  $^4\Phi$  state.

The geometrical structures obtained in the present calculations represent a wealth of information from which details of the bonding in transition-metal complexes can be understood. It is not possible to discuss all of these structures here, but some general aspects and some of the most noteworthy results will be mentioned. Most of the equilibrium structures are the expected ones. The two-coordinated systems have  $C_{2v}$  symmetry, the three-coordinated systems have  $C_{3v}$  or  $D_{3h}$  symmetry, and the four-coordinated systems have  $T_d$  symmetry. Most of the five-coordinated systems studied here have square-pyramidal symmetry and only some of them have the more expected trigonal-bipyramidal symmetry. The six-coordinated systems, finally, do not obtain octahedral symmetry but are distorted to a  $C_{3v}$  structure. The geometries of the transition states can all be rationalized in a simple way. The active  $\text{M}-\text{C}-\text{H}$  dissociating unit is very similar from system to system with a rather symmetric triangular shape with about equal  $\text{M}-\text{H}$  and  $\text{C}-\text{H}$  distances. The  $\text{CH}_4$  unit obviously adopts a rather tetrahedral structure, but what is perhaps less expected is that the orientation of the  $\text{MH}_x$  (or the  $\text{MH}_{x-1}\text{CH}_3$ ) unit is equally critical. It is energetically very important in most cases that the latter unit does obtain a structure, including the active dissociating hydrogen, that is similar to the optimal  $\text{MH}_{x+1}$  equilibrium geometry. For example, for the transition state of the reaction between  $\text{MH}_2$  and methane, the structure of the  $\text{MH}_3$  unit has to be pyramidal for ruthenium (see Figure 2, a and b) but planar for niobium (see Figure 2, c and d). In some cases an optimal structure of the  $\text{MH}_x\text{CH}_3$  unit is more important at

the transition state than an optimal  $\text{MH}_{x+1}$  unit (see for example Figure 2, e and f, for zirconium). For the reactions between  $\text{MH}_3$  and methane studied here, it was found that for similar reasons it is important that the  $\text{MH}_4$  unit is tetrahedral. For example, at the transition state of the reaction between  $\text{NbH}_3$  and methane (see Figure 1c), the rotation barrier for the  $\text{NbH}_3$  unit is as high as 20.8 kcal/mol.

The ground-state geometries of the two-coordinated complexes are all bent except for technetium. The reason for this is that technetium forms the only high-spin coupled two-coordinated complex to the right, which means that the bonds are formed from  $sp$  hybrids. For the low-spin two-coordinated complexes to the right the bonds are formed from  $sd$  hybrids and this leads to bond angles of approximately  $90^\circ$ . For the two-coordinated complexes to the left the bonding will be  $spd$  hybrids with bond angles between  $90$  and  $180^\circ$  depending on the amount of  $p$ - and  $d$ -character in the bonding. The reason for the efficient  $spd$  hybridization for the atoms to the left, in contrast to the case for the atoms to the right, is that the  $s^2$  state and the low-spin  $s^1$  state have the same spin for the atoms to the left.

For the three-coordinated complexes there is also an interesting difference between the atoms to the left and those to the right. The three-coordinated complexes to the left are planar while those to the right are nonplanar (see Figure 2, a and c). The energy difference between structures forced to be planar and the optimal nonplanar ones is quite large for the atoms to the right, 26.5 kcal/mol for  $\text{RhH}_3$ , for example. The origin of the planarity or nonplanarity of the three-coordinated complexes is best understood by first considering the bonding in the bent  $\text{MH}_2$  unit. The  $\text{M}-\text{H}$  bond of this unit in  $B_2$  symmetry is similar across the row for all metals but a significant difference appears for the  $\text{M}-\text{H}$  bond in  $A_1$  symmetry. For the atoms to the left from yttrium to niobium this bond is formed through  $sp$  hybridization, which is connected with the fact that  $s^2$  is the ground state or a low-lying state for these atoms. When the bonding  $sp$  hybrid is formed another  $sp$  hybrid will automatically form and this hybrid is in the plane of the  $\text{MH}_2$  subunit. This second hybrid will form the third  $\text{M}-\text{H}$  bond in  $\text{MH}_3$  and this system will therefore become planar for the atoms to the left. From the molybdenum complex and further to the right the  $\text{M}-\text{H}$  bond in symmetry  $A_1$  will be formed through  $sd$  hybridization rather than  $sp$  hybridization,

**Table II.** Reaction Energies (kcal/mol) for  $MH_x + H_2 + \Delta E \rightarrow MH_{x+2}$ 

metal (M)	x =				
	0	1	2	3	4
Y	-19.3	-24.0			
Zr	-19.7	-37.5	-41.3		
Nb	-16.4	-19.8	-22.8	-14.9	
Mo	2.5	-2.5	-6.6	1.0	-0.5
Tc	-2.7	-5.2	9.4	-0.7	
Ru	-11.4	-14.9	-14.8		
Rh	-23.8	-28.5			
Pd	-7.3				

which has been discussed more in detail in a recent paper.<sup>9f</sup> In the case of *sd* hybridization the second hybrid formed will instead point perpendicular to the  $MH_2$  plane. When the third M–H bond is formed in  $MH_3$  this system will therefore become nonplanar for the atoms to the right. If direct ligand–ligand repulsion plays any role for the geometries in the  $MH_x$  complexes it is probably only a minor one.

The five-coordinated complexes have only been optimized for niobium, molybdenum, and technetium. Most of these complexes obtained the square-pyramidal structure shown in Figure 1c, but  $MoH_5$  and  $TcH_5$  converged to distorted trigonal-bipyramidal structures shown in Figure 2g. For  $NbH_5$  the geometry search was started with a trigonal bipyramid but the convergence was downhill in energy all the way to the square-pyramidal structure, i.e. the same topological structure as in  $NbH_4CH_3$ . For the six-coordinated complexes, which were only studied for molybdenum, the geometry search was started from an octahedral structure. In this case the convergence was less straightforward than for the five-coordinated complexes, although still downhill, to the structure given in Figure 2d. This  $C_{3v}$  structure can be described as a piece of the fully coordinated optimal structure for  $ReH_9^{2-}$  and  $TcH_9^{2-}$ , a tricapped trigonal prism,<sup>15</sup> where three hydrogens are removed without changing the rest of the structure. It is interesting to note that this type of structure is commonly seen for electron deficient metal complexes such as  $Cr(CO)_x$  ( $x = 3, 4, 5$ ).<sup>16</sup>

The spin states for the transition states are in all cases, except for a few cases for technetium, the same as for the final products. For the reaction of  $TcH$  the spin at the transition state is lower than for the optimal product, whereas in the case of  $TcH_3$  the spin at the transition state is higher than for the product. The irregularity of the spin states for the technetium complexes makes these complexes harder to fit into the general pattern for the other metal complexes, and in most of the analysis below the technetium complexes are therefore excluded.

**b. Results for the Oxidative Addition of  $H_2$ .** The reaction energies for the oxidative addition reaction between  $MH_x$  and  $H_2$  are given in Table II for  $x$  from 0 to 4. The results are also displayed in Figure 3. All reactions, starting with the free metal atom and ending with the cases where all covalencies have been saturated, have been studied. The valence orbitals are the 4d and 5s orbitals. As an example of what this means, for yttrium with three valence electrons or rhodium with three valence holes in the 4d,5s shells, the complex which has saturated covalencies will have three hydride ligands. The largest number of ligands occurs for molybdenum with six valence electrons (and also six valence holes) and consequently with a possibility to bind six ligands covalently.

The largest reaction energies for the  $H_2$  addition reaction occur for the atoms to the left with  $ZrH_2$  as the extremum with 41.3 kcal/mol. As expected, on the basis of previous experience, the

(15) DeKock, R. L.; Gray, H. B. In *Chemical Structure and Bonding*; The Benjamin/Cummings Publishing Company, Inc.: Menlo Park, CA 1980; p 346.

(16) Elschenbroich, Ch; Salzer, A. *Organometallics*; VCH: Weinheim, 1992.

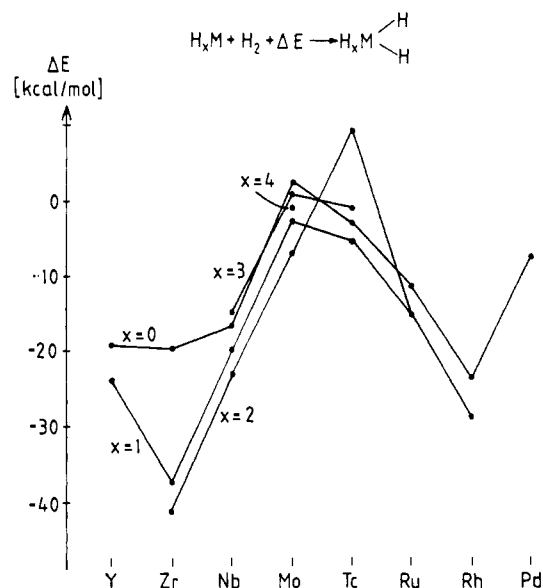


**Figure 3.** Energies for the  $H_xMH_2$  ( $x = 0-4$ ) insertion product calculated relative to the ground state of the  $H_xM$  ( $x = 0-4$ ) complex and free  $H_2$ . Negative values for  $\Delta E$  correspond to exothermic insertion reactions.

smallest reaction energies occur for the atoms in the middle of the row. The explanation for this is connected with the large loss of exchange energy when there are many unpaired 4d electrons, and this will be discussed further in subsection d below.

One rather surprising result that can be seen in Table II and Figure 3 is that the reaction energies for each metal are rather constant independent of the number of ligands, with a few exceptions. However, there are considerable differences between the different metals. The complexes of the atoms in the middle of the row, molybdenum and technetium, have reaction energies close to zero. Palladium has a reaction energy of about 10 kcal/mol, ruthenium one of about 15 kcal/mol, yttrium, niobium, and rhodium one of 20–25 kcal/mol, and finally zirconium one of about 40 kcal/mol. The simplest interpretation of these results is that the reaction energy should depend on the number of 4d electrons on the metal only. Clearly, this is a too simple description and ignores the effects of electronic promotion, loss of exchange energy, and steric effects. It would in fact be difficult by using an interpretation solely based on the number of 4d electrons to explain why the reaction energies should go through a minimum precisely in the region of molybdenum and technetium. It would also be difficult to explain the large difference in reaction energy between the Zr atom and  $ZrH$ , and it would be difficult to explain the difference between the reaction energies for  $NbH_2$  and  $NbH_3$ . Instead, a more detailed analysis is given in subsection d.

As seen in Table II, there are a few reaction energies close to zero. It should be pointed out that this does not necessarily mean that the potential surfaces for those complexes are very flat from this minimum out to reductive elimination of  $H_2$ . As already mentioned above, the reactant species is normally of higher spin than the product. In fact, when this is not the case a promotion energy for the reactant will enter the size of the reaction energy. The difference in spin between the reactant and product means that on the product potential energy surface there may very well be a quite deep minimum which leads to a well-defined geometry for the product. On this potential energy surface a very small or zero addition barrier is expected just as for the systems with large reaction energies.

**c. Results for the Oxidative Addition of  $CH_4$ .** The reaction energies for the oxidative addition reaction of  $CH_4$  to  $MH_x$  are given in Table III for  $x$  from 0 to 4 and also displayed in Figure 4. In general, the variation of the reaction energies for  $CH_4$  shows large similarities with the variation of the reaction energies for  $H_2$  in Table II and Figure 3, but the reaction energies are

**Table III.** Reaction Energies (kcal/mol) for  $\text{MH}_x + \text{CH}_4 + \Delta E \rightarrow \text{MH}_{x+1}\text{CH}_3^a$ 

metal (M)	x =				
	0	1	2	3	4
Y	-11.1	-14.5			
Zr	-12.8	-32.0	-37.9		
Nb	-10.4	-12.6	-18.4	-12.0	
Mo	12.1	4.9	-0.3	3.5	0.2
Tc	9.3	5.0	16.8	1.5	
Ru	3.9	-0.1	-4.7		
Rh	-6.5	-12.1			
Pd	9.3				

<sup>a</sup> The results for  $x = 0$  have been presented previously in ref 13c. The present values are 3.7 kcal/mol smaller than those in ref 13c since the correction for higher excitations is not included in the present paper.

**Table IV.** Difference in Reaction Energies (kcal/mol) between the  $\text{CH}_4$  and  $\text{H}_2$  Reaction Energies<sup>a</sup>

metal (M)	x =				
	0	1	2	3	4
Y	8.2	9.5			
Zr	6.9	5.5	3.4		
Nb	6.0	7.2	4.4	2.9	
Mo	9.6	7.4	6.3	2.5	0.7
Tc	12.0	10.2	7.4	2.2	
Ru	15.3	14.8	10.1		
Rh	17.3	16.4			
Pd	16.6				

<sup>a</sup> The  $\text{H}_2$  reactions are always more exothermic.

always smaller for the methane case. The smaller binding energy for the metal–methyl than for the metal–hydrogen bond is easiest explained by electron repulsion effects. The repulsion between the electrons on the metal and the larger number of electrons on methyl than on hydrogen results in a weaker binding energy for the metal–methyl bond. This is best seen on the difference in bond strength between the diatomic M–H and M–CH<sub>3</sub> bonds,<sup>11a</sup> which is much larger for the atoms to the right in line with the larger number of repulsive 4d electrons for these atoms than for the ones to the left. The largest reaction energy for the methane reaction is, just as for the  $\text{H}_2$  case, found for  $\text{ZrH}_2$ , and the reaction energies also go through a minimum for molybdenum and technetium. It is interesting to compare the reaction energies of  $\text{H}_2$  and  $\text{CH}_4$  in more detail, and therefore the differences in reaction energies are listed in Table IV. The first observation in Table IV is that the difference in reaction energies between  $\text{H}_2$  and  $\text{CH}_4$  tends to get smaller the more hydride ligands that are added. For example, for the Mo atom the difference in reaction energy between  $\text{H}_2$  and  $\text{CH}_4$  is 9.6 kcal/mol, which goes down to 7.4 kcal/mol for MoH, further down to 6.3 kcal/mol for MoH<sub>2</sub> and to 2.5 kcal/mol for MoH<sub>3</sub>, and finally down to 0.7 kcal/mol for MoH<sub>4</sub>. Another trend is that the difference in reaction energies between  $\text{H}_2$  and  $\text{CH}_4$  increases as one goes from left to right in the periodic table. For example, for the Zr and Nb atoms to the left this energy difference is 6–8 kcal/mol whereas for the atoms Ru–Pd it is 15–17 kcal/mol. These trends can be explained by steric and other repulsive effects (see further subsection d).

There are many ways to display the large number of results obtained in the present study. If the differences of the entries in Tables II and III are obtained, as given in Table IV, they show very systematic trends with a steady increase going from left to right in the periodic table and a steady decrease as more ligands are added. Exactly the same results can also be used to obtain still another table, namely that giving the reaction energies for the addition of  $\text{H}_2$  to  $\text{MCH}_3\text{H}_{x-1}$  for  $x$  from 1 to 4. These results can then be compared directly to the corresponding entries in Table II, which will then show the influence of exchanging a hydride ligand with a methyl group on the oxidative addition of  $\text{H}_2$ . Apart from some rather regular trends of this influence a few rather surprising results then emerge. For example, the

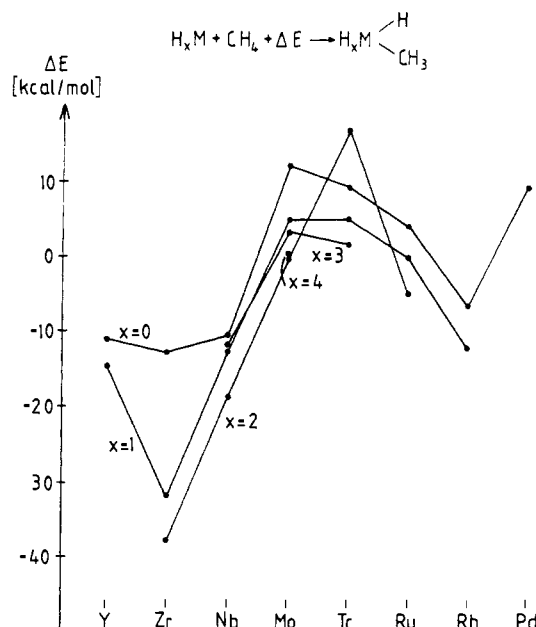


**Figure 4.** Energies for the  $\text{H}_x\text{MHCH}_3$  ( $x = 0-4$ ) insertion product calculated relative to the ground state of the  $\text{H}_x\text{M}$  ( $x = 0-4$ ) complex and free  $\text{CH}_4$ . Negative values for  $\Delta E$  correspond to exothermic insertion reactions.

reaction energy of adding  $\text{H}_2$  to  $\text{RuCH}_3$  is 3.6 kcal/mol smaller than that for adding  $\text{H}_2$  to  $\text{RuH}$ , while the reaction energy of adding  $\text{H}_2$  to  $\text{RuHCH}_3$  is 5.2 kcal/mol larger than that for adding  $\text{H}_2$  to  $\text{RuH}_2$ . It is clear that these results have to be explained by the same simple trends as described above for the difference in the reaction energies shown in Table IV, since they are based one exactly the same numbers. The main origin of the increase from -3.6 kcal/mol for  $\text{RuH}$  to +5.2 kcal/mol for  $\text{RuH}_2$  of exchanging a hydrogen with a methyl group is thus connected with the general decrease of the difference in the reaction energies in Table IV as the number of hydride ligands are increased. This trend is relatively straightforward to explain and this will be done in subsection d.

For the methane reaction, transition-state structures were obtained and the corresponding energies determined. These are given in Table V for the reaction between  $\text{MH}_x$  and  $\text{CH}_4$  for  $x$  from 0 to 4 and are also displayed in Figure 5. The lowest reaction barriers for the oxidative addition of methane are found for  $\text{RuH}_2$  with 2.0 kcal/mol,  $\text{RhH}$  with 6.7 kcal/mol, and  $\text{ZrH}_2$  with 7.7 kcal/mol. These are the only barriers lower than 10 kcal/mol in Table V. In a previous study,<sup>13c</sup> a calculation was performed at a higher level of accuracy for the reaction between the Pd atom and  $\text{CH}_4$ . This was a CCSD(T) (coupled cluster singles and doubles with a perturbational estimate of triples) calculation<sup>17</sup> using much larger basis sets than the ones used here. The effect of the higher accuracy was a lowering of the barrier by 4.4 kcal/mol of which 1.0 kcal/mol is a basis set effect and the rest a configuration effect. The binding energy of the insertion product was increased by 3.7 kcal/mol. It is most likely that similar effects also will be presented for all the other entries in Table III and V. If this is true,  $\text{RuH}_2$  will thus, as the only system studied here, not have any barrier for the oxidative addition of  $\text{CH}_4$ .

When reaction barriers are discussed it is common to discuss these in terms of a thermodynamic driving force. For example, it is clear that the low barrier of  $\text{ZrH}_2$  of 7.7 kcal/mol is connected with the large exothermicity of 37.9 kcal/mol (the largest of all of the presently studied systems) for the methane reaction. However, from the present results it is also clear that the low

(17) The coupled cluster calculations are performed using the TITAN set of electronic structure programs, written by Lee, T. J., Rendell, A. P., Rice, J. E.

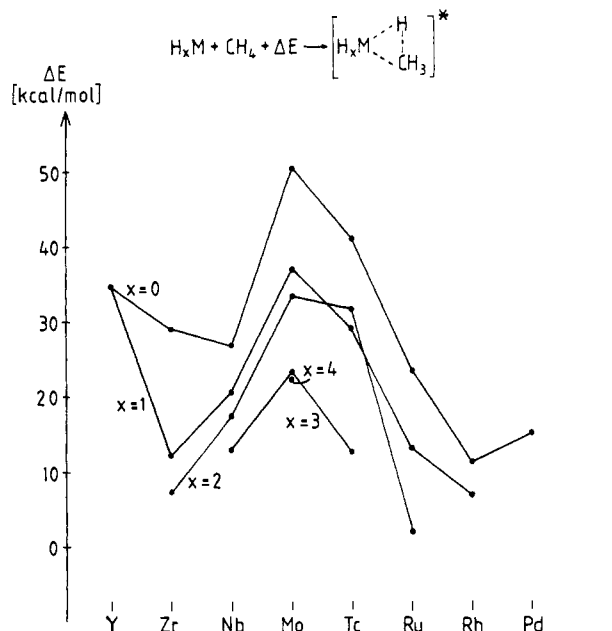


Figure 5. Transition-state energies of C-H activation of methane calculated relative to the ground state of the  $H_xM$  ( $x = 0-4$ ) complex and free  $CH_4$ . Negative values for  $\Delta E$  corresponds to barrierless insertion reactions.

Table V. Barrier Heights (kcal/mol) for  $MH_x + CH_4 + \Delta E \rightarrow MH_{x+1}CH_3^a$

metal (M)	x =				
	0	1	2	3	4
Y	34.4	34.4			
Zr	29.0	12.1	7.7		
Nb	26.6	20.5	17.7	12.8	
Mo	50.7	37.1	33.7	23.3	22.7
Tc	41.1	28.9	31.8	12.2	
Ru	23.4	13.0	2.0		
Rh	11.2	6.7			
Pd	15.0				

<sup>a</sup> The results for  $x = 0$  have been presented previously in ref 13c. The present values are 4.4 kcal/mol higher than those in ref 13c since the correction for higher excitations is not included in the present paper.

barriers for the complexes of the atoms to the right, such as for  $RuH$  and  $RuH_2$ , have to be explained by other factors than the exothermicities which are not particularly high. Instead, the origin of these low barriers is explained by the presence of low-lying  $s^0$  states. As emphasized in previous studies,<sup>13</sup> this is the state with the least repulsion toward ligands and it allows the metal to approach methane close enough to effectively interact with the C-H bond. The  $s^0$  state is of the wrong spin to mix into the wave function for the complexes to the left and therefore in general these have higher barriers than those to the right. For the atoms to the left, the  $s^2$  and  $sp$  states will instead mix into the wave function. This is a contributing factor for the large reaction energies to the left, but this mixing is not very effective in the transition-state region. For example, for the complexes of yttrium, which has an  $s^2$  ground state, there will be large contributions from this state. This leads to relatively large exothermicities for the yttrium complexes but also to some of the highest barriers of the systems studied here, due to the large repulsion from almost two  $sp$  electrons.

It is interesting to note that the  $Rh(I)$  complex ( $RhH$ ) studied here has one of the lowest barriers (in fact only  $RuH_2$  has a lower barrier). This result is in line with present experimental findings where so far only  $Rh(I)$  complexes of the second-row transition-metal complexes have been found to be active in breaking the C-H bond of alkanes. It is clear that confirmative comparisons of this kind represent the basis for the present type of more

Table VI. Promotion and Exchange Energies (kcal/mol) for  $MH_x + H_2 \rightarrow MH_{x+2}$

metal (M)	x =				
	0	1	2	3	4
Y	49.1	27.4			
Zr	40.8	21.9	6.5		
Nb	38.3	35.5	21.3	7.1	
Mo	51.4	53.6	38.3	23.0	7.7
Ru	28.4	25.7	8.6		
Rh	16.3	9.0			
Pd	24.0				

systematic theoretical approaches toward the understanding of these reactions.

**d. Analysis of the Results.** In this subsection the results in Tables II-V will be analyzed in terms of the major effect present in the reactions. Some of these effects have already been mentioned. It is clear that whenever covalent bonds are formed it may be necessary to make an electronic promotion of the reactant to a state with a sufficient number of open shell orbitals, i.e.  $x$  more than in the final product, where  $x$  is the number of covalent bonds formed. For example, such a promotion effect is the simplest explanation for the fact that the Pd atom has a smaller reaction energy than the Rh atom. The Pd atom has a  $4d^{10}$  ground state without open shells and needs to be promoted to the lowest state with two open shells, the  $4d^9 5s^1$  state, for the oxidative addition of  $H_2$  or  $CH_4$ . No such promotion is necessary for the Rh atom which already has a ground state that has two open shell orbitals. There are only five reactions studied here where a promotion effect is necessary. These cases have already been mentioned and the promotion energies were given in subsection a. The cases are the Y atom, the Zr atom, the Pd atom, and the diatomic molecules  $YH$  and  $ZrH$ .

The second major effect present in the reactions is the loss of exchange energy when the two new bonds are formed in the product. This energy loss is largest for the cases where the reactant has a large number of open shells. The maximum number of open  $4d$  orbitals occurs for the atoms in the middle of the row, molybdenum and technetium, and a minimum in the reaction energies is therefore seen for these atoms. This exchange energy loss has been mentioned in many previous studies, most notably by Carter and Goddard,<sup>14</sup> who have also tabulated exchange integrals which can be used to quantitatively estimate the size of these energy losses. These integrals were given for the case of transition-metal cations and not for neutral atoms, which should ideally have been used for the present analysis. However, first these integrals are not expected to be very different for the neutral atoms, and second it should be clear that a perfect quantitative analysis of the present results will not be achieved anyway by this rather simple analysis. The cationic integrals will therefore suffice well for the present purpose. The state chosen in the table for these integrals in ref 14 was taken to be the cationic state with the same occupation as the  $s^1$  neutral state. For example, for Zr the choice of state was the  $4d^3 5s^1$  state of the  $Nb^+$  cation. After that it is trivial to obtain the exchange energy losses in the addition reaction which are given in Table VI, where also the five promotion energies from subsection a have been added. The entries in this table are as can be seen rather large, in particular for the least ligated complexes toward the middle of the periodic table. The entry for the yttrium atom is also very large, which is due to an unusually large promotion energy.

In Tables VII-IX, the promotion and exchange energies from Table VII have been added to the entries in Tables II, III, and V (except for technetium which represents a special case and is withdrawn from the present analysis). If these effects were the only important energetic effects present in the reactions, all entries in each of the Tables VII-IX should be the same. However, as seen from these tables this is not the case. In some cases the promotion and exchange corrections are very successful. For

**Table VII.** Reaction Energies (kcal/mol) minus Promotion and Exchange Energies for  $MH_x + H_2 + \Delta E \rightarrow MH_{x+2}$ 

metal (M)	x =				
	0	1	2	3	4
Y	-68.4	-51.4			
Zr	-60.5	-59.4	-47.8		
Nb	-54.7	-55.3	-44.1	-22.0	
Mo	-48.9	-56.1	-44.9	-22.0	-8.2
Ru	-39.8	-40.6	-23.4		
Rh	-40.1	-37.5			
Pd	-31.3				

**Table VIII.** Reaction Energies minus Promotion and Exchange Energies (kcal/mol) for  $MH_x + CH_4 + \Delta E \rightarrow MH_{x+1}CH_3$ 

metal (M)	x =				
	0	1	2	3	4
Y	-60.2	-41.9			
Zr	-53.6	-53.9	-44.4		
Nb	-48.7	-48.1	-39.7	-19.1	
Mo	-39.3	-48.7	-38.6	-19.5	-7.5
Ru	-24.5	-25.8	-13.3		
Rh	-22.8	-21.1			
Pd	-14.7				

**Table IX.** Barrier Heights minus Promotion and Exchange Energies (kcal/mol) for  $MH_x + CH_4 + \Delta E \rightarrow MH_{x+1}CH_3$ 

metal (M)	x =				
	0	1	2	3	4
Y	-14.7	7.0			
Zr	-11.8	-9.8	1.2		
Nb	-11.7	-15.0	-3.6	5.7	
Mo	-0.7	-16.5	-4.6	0.3	15.0
Ru	-5.0	-12.7	-6.6		
Rh	-5.1	-2.3			
Pd	-9.0				

example, the difference between the reaction energies of  $H_2$  for the Zr atom and ZrH has been reduced to 1.1 kcal/mol from 17.8 kcal/mol. In other cases there is a moderate success, such as for the difference between the Pd atom and the Rh atom, where the difference has been reduced from 16.5 kcal/mol to 8.8 kcal/mol. Also, the minimum in the reaction energies in the middle of the row for molybdenum has been removed. However, as a whole it is clear that other important energetic effects also are present in the reactions.

One thing that the corrections from Table VI have done is to make the trends of the remaining effects more clear. If we focus on the reaction energies in Table VII and VIII, then with a few exceptions these effects can be described by two systematic trends. The first of these trends is the systematic decrease of the reaction energies as one goes from left to right in the periodic table. The second trend is a systematic decrease of the reaction energies as more ligands are added. The origins of these trends are relatively easy to understand. The origin of the first trend is the repulsion between the electrons on the metal and the electrons on the added  $H_2$  or  $CH_4$ . It is clear that this repulsion should be largest for the atoms with the largest number of 4d electrons to the right, and this leads to smaller reaction energies for these atoms. The origin of the second trend is a more direct steric repulsion between the different ligands, which is also combined with a rehybridization effect on the metal (see further below). This steric effect should obviously be larger the more ligands that are present.

An interesting result, which has already been mentioned in subsection b, is given by the difference in reaction energies for  $H_2$  and  $CH_4$  given in Table IV and supports the above identification of the major energetic effects. It should be added that this difference is not modified by the addition of the corrections from Table VI, since the corrections are identical for

$H_2$  and  $CH_4$ . There are two trends for this energy difference. The first trend is that the difference tends to get larger for the atoms to the right. The second trend, which is perhaps counterintuitive, is that the difference tends to get smaller the more ligands that are added. Both of these trends go logically together with the fact that the repulsion between the metal electrons and the ligand electrons is a dominant effect. Since there are more 4d electrons to the right and methyl has more electrons than hydrogen, the difference in the reaction energy between  $H_2$  and  $CH_4$  should be larger for the atoms to the right, which explains the first trend. The second trend is explained by the same origin as the first trend and the fact that the ligands are electronegative. The more ligands that are added the more electrons will be moved away from the metal, and the repulsion between the metal and the ligands will therefore be smaller. Since it is this repulsion that causes the difference in the reaction energies between  $H_2$  and  $CH_4$ , a decrease in this repulsive effect will tend to make this difference smaller. There should be a compensating effect in that the direct steric repulsion between methyl and the hydrogen ligands should be larger than the ones between hydrogen ligands, but this effect is, perhaps surprisingly, quite small (see further below).

The results in Tables VII and VIII make it possible to quantify the steric and other repulsive effects of adding ligands for the oxidative addition reaction. Starting from the reaction energy for the atoms and adding ligands it can be seen that the first ligand has a very small effect on the energetics. The steric and repulsive effect for the first ligand can be quantified as 0 kcal/mol. The addition of the second ligand causes a general decrease of the reaction energies by approximately 10 kcal/mol. The third ligand leads to an additional decrease of 20 kcal/mol, and finally the fourth ligand leads to an additional decrease of 15 kcal/mol. It should be added that these energies are practically the same for the  $H_2$  and  $CH_4$  reaction. The general change of the steric and repulsive effects can be explained by two dominating effects. There is first a direct negative effect on the reaction energy from increasing the number of ligands. It is tempting to describe this effect as a steric repulsion effect between the ligands. But since the effect is almost identical for  $H_2$  and  $CH_4$  this effect is perhaps better described as a rehybridization effect on the metal. A rehybridization effect should only depend on the number and the direction of the bonds. For example, it is clear that going from the tetrahedral structure of  $NbH_4$  to the square-pyramidal structure of  $NbH_5$ , a considerable rehybridization energy is required. The difference between the reaction energies for  $NbH_2$  and  $NbH_3$  with  $H_2$  is therefore as large as 22 kcal/mol. It is also clear that the rehybridization energy difference between  $NbH_2$  and  $NbH_3$  should be quite small. The bonds can be formed with essentially already available hybrids. The difference between the reaction energies for the Nb atom and  $NbH$  is therefore almost zero. For the difference in reaction energies as the number of ligands is increased, the change in direct repulsion between the electrons on the metal atom and the ligands also has an influence. This is best seen, as has already been discussed, from the fact that the difference in reaction energy between  $H_2$  and  $CH_4$  steadily decreases as the number of ligands is increased. The more electronegative ligands that are added the more electrons are removed from the metal, and this causes a gradual decrease of this repulsive effect.

It is perhaps worthwhile to consider in more detail the possibility that direct ligand-ligand repulsion plays an important role for the trends in Tables VII and VIII. One argument against that is that the trends in the reaction energies of adding ligands are so extremely similar between the  $H_2$  and  $CH_4$  reactions. Intuitively one could have expected that the ligand repulsion effects should have been substantially larger for the  $CH_4$  reaction, since the methyl group is both larger and contains more electrons than the hydrogen atom. But if this intuitive argument is disregarded,

then perhaps the rest of the results might be consistent with strong ligand–ligand repulsion effects. To investigate this possibility the results for the H<sub>2</sub> reaction in Table VII can be studied in detail. If repulsive ligand effects are dominant these effects are expected to be more or less directly dependent on the number of ligand pairs. Since the number of ligand pairs increases quadratically with the number of ligands, the number of new ligand pairs formed in the reaction with H<sub>2</sub> increases linearly with the number of added ligands. Therefore the differences between the entries for consecutive  $x$  values for the same metal in Table VII should be the same. This prediction is contradicted everywhere in this table. First, the difference between  $x$  equals 0 and 1 is almost 0, while the difference between  $x = 1$  and 2 is 10 kcal/mol. This could, of course, be a consequence of the fact that with very few ligands present the ligands could avoid each other and thereby reduce the repulsive effect. However, also this possibility is contradicted by the results for  $x = 4$ , where the decrease in energy is suddenly smaller than it was for  $x$  equals 3. There are consequently no clear indications of important direct ligand–ligand repulsion effects in the results of the present study. However, this situation might be different for more bulky and even more electronegative ligands than the ones used in the present study, and the situation should be reinvestigated for these cases.

There is one metal for which correction from exchange and promotion effects has not worked at all, and this is for yttrium. Before the correction is added the reaction energies for the Y atom and YH are rather similar with values of 19.3 and 24.0 kcal/mol. After the correction is added the reaction energies are much more different with values of 68.4 and 51.4 kcal/mol. The origin of this failure is probably the use of unrealistic promotion energies. The promotion energy for the yttrium atom is 34.1 kcal/mol, but for YH the promotion energy is only 21.6 kcal/mol. It has already been mentioned that a complicating factor is that the yttrium atom has a second excited state which is appropriate for binding with a promotion energy of 39.7 kcal/mol, which is quite close to the promotion energy to the lowest bonding state. This probably leads to an effectively smaller promotion energy than any of these two excitation energies. Another complicating factor is that the bonding for the atoms to the left is quite ionic. If the analysis would have started out from a completely ionic bonding it is clear that the values for promotion and exchange energy losses would have been quite different. It is thus not trivial exactly how an appropriate analysis should be carried out in each case, and the case of yttrium can here serve as an example of where the most straightforward analysis has not been completely successful.

A few comments should be made on the exchange and promotion corrected barrier heights given in Table IX. First, all but a few of these barrier heights are below 0. This should not be interpreted as if this situation could be achieved for the complex of any second-row metal if the appropriate ligands were chosen. For any complex there always has to be at least an exchange energy loss since two new bonds are formed in the addition reaction. A second comment is that even though the corrections from Table VI are sometimes less successful, in general, the reduced loss of exchange is a useful explanation for the fact that the barriers tend to get lower as more ligands are added. One example where the addition of exchange and promotion energy has been quite successful is found for the difference between the Zr atom and ZrH where the difference in barrier heights has been reduced to 2.0 kcal/mol from 16.9 kcal/mol. Another such example is the difference between the barriers for the Ru atom and the Rh atom, where the difference is reduced from 12.2 kcal/mol to 0.1 kcal/mol. Another comment on the results in Table IX is that for some of the complexes of the atoms in the middle of the row, such as for MoH, the results seem to indicate that the complexes of these atoms should be the most effective in the oxidative addition reaction for CH<sub>4</sub>. However, this is

contradicted by the results in the table for some of the larger complexes like MoH<sub>3</sub>. These examples show some of the limitations of the present type of analysis for the barrier heights. One reason for this is that certain electronic states which have not entered the analysis are very important at the transition states. In particular, the presence of a low-lying  $s^0$  state is found to be of key importance for a low activation barrier. At present it is not clear exactly how this excited state should enter the quantitative analysis of the results, and this part of the analysis is therefore left at this point.

### III. Conclusions

Previous systematic theoretical studies of bonding and reactivity of second-row transition metals have in most cases not included ligands on the metal atom.<sup>13</sup> These studies have identified the importance of different electronic structure effects, such as the mixing between different electronic states and the need to promote some of the metals to excited states before the reaction. The important role of the loss of exchange energy in the oxidative addition reaction has also been pointed out.<sup>13,14</sup> An explanation for the larger size of the barrier for the addition of CH<sub>4</sub> compared to the addition of H<sub>2</sub> has also been given in terms of the directionality of the methyl group.<sup>9,10</sup> The present study of ligated metal complexes has given a closer insight into some of these effects and also allowed the identification of some other important energetic effect in the oxidative addition reaction.

Without addition of promotion and exchange effects the reaction energies for the oxidative addition reaction go through a minimum for the metals in the middle of the row. After the addition of these effects two new trends can be identified. First, there is a systematic decrease of the reaction energies as one goes from left to right in the periodic table. This trend is explained by the dominant role of electron repulsion between the metal electrons and the ligand electrons, which increases with the increasing number of metal electrons to the right in the row. The second trend is a systematic decrease of the reaction energies as the number of hydrogen ligands is increased. This trend is intuitively explained simply by the direct steric repulsion effects between the ligands. However, since this effect is practically identical for the H<sub>2</sub> and CH<sub>4</sub> reactions it appears that the effect is dominated by local rehybridization on the metal, which should be the same for hydrogen and methyl ligands.

The comparison between the H<sub>2</sub> and CH<sub>4</sub> reactions provide additional insight into the dominating energetic effects in the oxidative addition reaction. The difference between the reaction energies for these reactions increases to the right in the periodic table. This trend is again best explained by the important role of the electronic repulsion effect between the metal electrons and the electrons on the ligands. Methyl has more electrons than hydrogen and this repulsion is therefore larger for methyl and larger to the right in the periodic table, which leads to an increased difference between the reaction energies of H<sub>2</sub> and CH<sub>4</sub> to the right. The second trend in the difference between the reaction energies of H<sub>2</sub> and CH<sub>4</sub> is more surprising. Even though methyl is bulkier than the hydrogen atom, the difference in reaction energy between H<sub>2</sub> and CH<sub>4</sub> decreases as the number of ligands increases. This counterintuitive trend is explained by the electronegative character of the hydrogen and methyl ligands. This means that as more ligands are added more electrons are moved from the metal to the ligands, which in turn means that the direct repulsive effect between the electrons on the metal and the electrons on the ligands should decrease. Since this repulsive effect is the dominating origin of the difference in the reaction energies between H<sub>2</sub> and CH<sub>4</sub>, this difference will also decrease as more ligands are added.

The lowest barriers obtained for the oxidative addition of methane are of particular interest in comparison to what is known experimentally. The second lowest barrier of all reactions studied



here is obtained for RhH, which is a Rh(I) complex. This is in line with the fact that the only second-row transition-metal complexes which are found to dissociate the C-H bond in alkanes are Rh(I) complexes. However, the lowest barrier for this reaction obtained in the present study actually occurs for RuH<sub>2</sub>. In fact, when corrections for a larger basis set and configuration expansion are made, RuH<sub>2</sub> is predicted not to have any barrier for this reaction. This result should hopefully inspire further investigations of the oxidative addition reaction of alkanes with particular focus on Ru(II) complexes.

#### Appendix: Computational Details

In the calculations reported in the present paper for the oxidative addition of methane and the hydrogen molecule to second-row transition-metal atoms and complexes, reasonably large basis sets were used in a generalized contraction scheme<sup>18</sup> and all valence electrons were correlated using size consistent methods.

For the metals the Huzinaga primitive basis<sup>19</sup> was extended by adding one diffuse d-function, two p-functions in the 5p region, and three f-functions, yielding a (17s,13p,9d,3f) primitive basis. The core orbitals were totally contracted<sup>18</sup> except for the 4s and 4p orbitals which have to be described by at least two functions each to properly reproduce the relativistic effects.<sup>20</sup> The 5s and 5p orbitals were described by a double- $\zeta$  contraction and the 4d by a triple- $\zeta$  contraction. The f functions were contracted to one function giving a [7s,6p,4d,1f] contracted basis. For carbon the primitive (9s,5p) basis of Huzinaga<sup>21</sup> was used, contracted according to the generalized contraction scheme to [3s,2p], and one d-function with the exponent 0.63 was added. For hydrogen the primitive (5s) basis from ref 2 was used, augmented with one p-function with the exponent 0.8 and contracted to [3s,1p]. These basis sets were used in the energy calculations for all systems.

In the geometry optimizations, performed at the SCF level as described below, somewhat smaller basis sets were used. For the metals a relativistic ECP according to Hay and Wadt<sup>22</sup> was used. The frozen 4s and 4p orbitals are described by a single- $\zeta$  contraction, the valence 5s and 5p orbitals are described by a double- $\zeta$  basis, and the 4d orbital is described by a triple- $\zeta$  basis, including one diffuse function. The rest of the atoms are described by standard double- $\zeta$  basis sets.

The correlated calculations were performed using the modified coupled pair functional (MCPF) method,<sup>23</sup> which is a size-consistent, single-reference-state method. The zeroth order wave functions are determined at the SCF level. The metal valence electrons (4d and 5s) and all electrons on the hydrogen and methane units except the carbon 1s electrons were correlated. To judge the absolute accuracy of the calculations is rather difficult since no accurate experimental information is available for the present systems. However, in a previous study on the oxidative addition of methane an investigation of the accuracy was made using much larger basis sets and a correlation treatment including triple excitations.<sup>13c</sup> It was then found that the insertion barrier is lowered by 4.4 kcal/mol, of which 1.0 kcal/mol is a basis effect and 3.4 kcal/mol an effect of triple excitations. The binding energy of the insertion products is correspondingly increased by 3.7 kcal/mol, of which 1.5 kcal/mol is a basis set effect and 2.2 kcal/mol is the effect of triple excitations. The results of these more accurate calculations should be within a few kcal/mol of the exact limit. It can also be noted that the relative energy between the insertion product and the transition state is rather stable at these different levels of treatment.

In the correlated calculations relativistic effects were accounted

(18) (a) Almlöf, J.; Taylor, P. R. *J. Chem. Phys.* **1987**, *86*, 4070. (b) Raffenetti, R. C. *J. Chem. Phys.* **1973**, *58*, 4452.

(19) Huzinaga, S. *J. Chem. Phys.* **1977**, *66*, 4245.

(20) Blomberg, M. R. A.; Wahlgren, U. *Chem. Phys. Lett.* **1988**, *145*, 393.

(21) Huzinaga, S. *J. Chem. Phys.* **1965**, *42*, 1293.

(22) Hay, P. J.; Wadt, W. R. *J. Chem. Phys.* **1985**, *82*, 299.

(23) Chong, D. P.; Langhoff, S. R. *J. Chem. Phys.* **1986**, *84*, 5606.

for by using first-order perturbation theory including the mass-velocity and Darwin terms.<sup>24</sup>

The geometries for all systems were fully optimized at the SCF level, for both equilibrium and transition-state structures. The optimizations were performed using the GAMESS program.<sup>25</sup> A C<sub>v</sub> symmetry constraint was used in some of the optimizations. In these cases the rotation of the methyl group was fixed, which should affect the energy by certainly less than 1 kcal/mol. However, it should be noted that any conclusion eclipsed or staggered orientations of the C-H bonds with respect to the M-H bonds cannot be drawn for these systems.

A few words should be said about the level of calculation chosen in the present study. As described above the geometries are optimized at the SCF level and the relative energies are calculated at the MCPF level, i.e. electron correlation effects are included. First, it should be emphasized that the correlation effects on both the reaction energies and the barrier heights are large. In particular, the size of the correlation effects varies strongly across the periodic table so that the diagrams shown in the figures would have appeared very differently if SCF results had been used instead of correlated results. A detailed discussion of correlation effects on metal-ligand binding energies is given in ref 26. The conclusion is that correlation effects have to be included in the calculations to give reliable trends for activation energies and binding energies. Secondly, it can be questioned if the use of SCF-optimized geometries gives reliable results, in particular since the correlation effects are so large. There are several results on systems similar to those studied in the present paper showing that SCF-optimized and MCPF-optimized geometries give very similar relative energies. For example, it was shown in ref 13b for the methane activation reaction that the barrier height for rhodium, the metal with the largest correlation effects in the present context, changed by less than 1 kcal/mol on going from an SCF- to an MCPF-optimized geometry. Also, it is the experience of Bauschlicher and co-workers<sup>27</sup> that if a consistent set of ligand and metal-ligand geometries is used, the binding energies calculated at the MCPF level agree to better than 1 kcal/mol, regardless of whether the equilibrium structures are optimized at the SCF or MCPF level of theory. The origin of this surprising behavior is that in the most interesting region of the potential energy surfaces (including both the transition state and the insertion products) and SCF and the MCPF surfaces are quite parallel. This is seen on the rather small correlation effects on the elimination barriers. For example, for the barrier of ethylene elimination from palladium vinyl hydride<sup>13c</sup> the SCF and the MCPF values are identical, and for the corresponding rhodium reaction the correlation effects lower the elimination barrier by only 4 kcal/mol, compared to 56 kcal/mol for the activation barrier. Another reason SCF geometries can be used is that the potential energy surfaces are often rather flat in both the transition-state region and the insertion product region, so that discrepancies in SCF- and MCPF-optimized structures have very small effects on the relative energies. The conclusion is that the use of SCF-optimized structures gives reliable results for the trends in activation energies and binding energies if correlation effects are included in the energy calculations.

Finally, a general and rather complex question will be addressed. In the reactions studied in the present paper the ground state of the reactants normally has a higher total spin than the ground

(24) Martin, R. L. *J. Phys. Chem.* **1983**, *87*, 750. See also: Cowan, R. D.; Griffin, D. C. *J. Opt. Soc. Am.* **1976**, *66*, 1010.

(25) GAMESS (General Atomic and Molecular Electronic Structure System): Schmidt, M. W.; Baldridge, K. K.; Boatz, J. A.; Jensen, J. H.; Koseki, S.; Gordon, M. S.; Nguyen, K. A.; Windus, T. L.; Elbert, S. T. *QCPE Bull.* **1990**, *10*, 52.

(26) Blomberg, M. R. A.; Siegbahn, P. E. M.; Svensson, M. *J. Phys. Chem.* **1992**, *96*, 9794.

(27) (a) Sodupe, M.; Bauschlicher, C. W., Jr.; Langhoff, S. R.; Partridge, H. *J. Phys. Chem.* **1992**, *96*, 2118. (b) Rosi, M.; Bauschlicher, V. W., Jr. *Chem. Phys. Lett.* **1990**, *166*, 189. (c) Bauschlicher, C. W., Jr.; Langhoff, S. R. *J. Phys. Chem.* **1991**, *95*, 2278.

state of the products. Two comments can be made in this context. First, the question whether the binding energies should be given relative to reactants with the same spin as the products or relative to the spin of the ground-state reactants is mainly a pedagogical problem. One set of energies can be easily transferred to the other set using available excitation energies. The common praxis has been to always relate to the energies for the ground spin states of the reactants, see for example ref 10–12. The main advantage with this praxis is that the procedure is easily defined. A more serious question concerning the spin states of the reactions is what actually happens dynamically during the reaction. If the reaction starts with ground-state reactants and ends up with ground-state products, the spin has to change through a spin-orbit effect. These effects are known to be strong for transition metals so this surface hopping will probably occur with a high

probability. Since the potential surface for the high-spin reactants is normally strongly repulsive, the crossing between the two spin surfaces will in most cases occur far out in the reactant channel, long before the saddle point of the reaction is reached. This is at least true in the most interesting cases where the low-spin surface of the reactants is not too highly excited. For the oxidative addition reaction this assumption is, for example, confirmed by calculations by Balasubramanian.<sup>28</sup> This means that the probability for surface hopping through spin-orbit coupling will affect the pre-exponential factor of the rate constant but not the size of the barrier. The presently computed barrier heights should therefore in most cases be directly comparable to experimental measurements of activation energies.

---

(28) Balasubramanian, K.; Liao, D.-W. *J. Phys. Chem.* **1988**, *92*, 6259.